

Microtubule biopolymers: fibre diffraction and effects of interparticle scattering

W. Bras¹, G.P. Diakun², R.C. Denny², A. Gleeson², C. Ferrero³, Y.K. Levine⁴ and J. F. Díaz⁵

¹ Netherlands Organisation for Scientific research (NWO) DUBBLE CRG/ESRF BP 220 F38043 Grenoble Cedex France

² CLRC Daresbury Laboratory, Daresbury, Warrington, Cheshire WA4 4AD, U.K.

³ European Synchrotron Radiation Facility BP 220 F38043 Grenoble Cedex France

⁴ Utrecht University Molecular Biophysics PO Box 20000 Utrecht Netherlands

⁵ KU Leuven, Laboratory for Chemical and Biological Dynamics, Celestijnenlaan 200 D, Leuven, Belgium

Introduction

Microtubules play several important roles in the cell [1]. They consist of long chains of tubulin protein dimers, called protofilaments, which connect laterally to form a hollow cylindrical structure with an external diameter of approximately 30 nm and a length which can extend to microns. The number of protofilaments can vary, but the predominant number in a normal functioning cell is 13. The persistence length of these polymers is reported to be between 2000 and 5200 μm [2,3], so that for most experiments they can be considered to be a monodisperse rigid rod system with a large polydispersity in the length. In the experiments described here the average length is approximately 5 μm [4] giving an average molecular weight of 10^9 Dalton.

The preparation of hydrated microtubule samples suitable for small angle X-ray fibre diffraction is not trivial. A reasonably successful method has been centrifugation over extended lengths of time (>24 hours) and subsequent rehydration [5]. We have developed a less invasive method using the cooperative effect of the diamagnetic moment of the tubulin dimers in combination with strong magnetic fields to induce orientation on microtubules in diluted solutions. For rigid rod molecules with an axial ratio of 50 - 200 without any constraint applied to them, Flory has predicted that the angular distribution of the long axis would be at most 10.2 -

- Booth, C., *Macromolecules* (1998) **20**, 6958-6963.
- [25] Mortensen, K., Brown, W., Almdal, K., Alami, E. and Jada, A., *Langmuir* (1997) **13**, 3635-3645.
- [26] Mortensen, K., Brown, W. and Jorgensen, E., *Macromolecules* (1994) **27**, 5654-5666.
- [27] Mortensen, K., *Macromolecules* (1997) **30**, 503-507.
- [28] Zhou, Z.K., Chu, B. and Nace, V.M., *Langmuir* (1996) **12**, 5016-5021.
- [29] Zhou, Z.K., Chu, B., Nace, V.M., Yang, Y.W. and Booth, C., *Macromolecules* (1996) **29**, 3663-3664.
- [30] Yang, Y.W., Yang, Z., Zhou, Z.K., Attwood, D. and Booth, C., *Macromolecules* (1996) **29**, 670-680.
- [31] Chu, B. and Wu, G.W., *Macromolecular Symposia* **87**, 55-67.
- [32] Alexandridis, P., Olsson, U. and Lindman, B., *Macromolecules* (1995) **28**, 7700-7710.
- [33] Wu, G.W., Liu, L.Z., Buu, V.B., Chu, B. and Schneider, D.K., *Physica A* (1996) **231**, 73-81.
- [34] Alexandridis, P., Olsson, U. and Lindman, B., *Langmuir* (1996) **12**, 1419-1422.
- [35] Lairez, D., Adam, M., Raspaud, E., Carton, J.P. and Bouchaud, J.P., *Macromolecular Symposia* (1995) **90**, 203-229.
- [36] Raspaud, E., Lairez, D., Adam, M. and Carton, J.P., *Macromolecules* (1996) **29**, 1269-1277; *Macromolecules* (1994) **27**, 2956-2964.
- [37] Mischenko, N., Reynders, K., Koch, M., Mortensen, K., Pedersen, J.S., Fontain, F., Graulus, R. and Reynaers, H., *Macromolecules* (1995) **28**, 2054-2062.
- [38] Mischenko, N., Reynders, K., Scherrenberg, R., Mortensen, K., Fontain, F., Graulus, R. and Reynaers, H., *Macromolecules* (1994) **27**, 2345-2347.
- [39] Laurer, J.H., Bukovnik, R. and Spontak, R.J., *Macromolecules* (1996) **29**, 5760-5762.
- [40] Reynders, K., Mischenko, N., Mortensen, K., Overbergh, N. and Reynaers, H., *Macromolecules* (1995) **28**, 8699-8701.
- [41] Mischenko, N., Reynders, K., Mortensen, K., Overbergh, N. and Reynaers, H., *J. Polym. Science: B. Polym. Phys.* (1996) **34**, 2739-2745.
- [42] Kleppinger, R., Reynders, K., Mischenko, H., Overbergh, N., Koch, M.H.J., Mortensen, K. and Reynaers, H., *Macromolecules* (1997) **30**, 7008-7011.
- [43] Kleppinger, R., Mischenko, H., Reynaers, H., Koch, M.H.J., Almdal, K. and Mortensen, K., *Macromolecules* (1997) **30**, 7012-7014.

11° [6,7]. This prediction has been confirmed by our earlier experiments [8]. The analysis of the fibre diffraction pattern is therefore rather difficult since the degree of alignment is such that at higher q -values the reflections belonging to the layer lines can start to overlap with the diffraction arcs from the equator or other layer lines. In Figure 1 the diffracted intensity on the equator and the first layer line is shown. To obtain these curves it was necessary to correct for the disorientation and several geometrical parameters. For this the CCP13 suite of software was used [8, 9, 10]. Due to the longitudinal staggering of the different protofilaments, the surfaces of microtubules have shallow helical grooves running over them so that the diffraction pattern has to be explained in terms of helical diffraction theory [11,12].

In order to increase the accuracy and to avoid software induced systematic errors for the intermediate order diffraction peaks, a different method has been tried. In this case the microtubules

were aligned with their axis parallel to the X-ray beam. This means that one only observes the scattering pattern from the equatorial plane and thus avoids the overlap between the different reflections at least until the resolution where higher order layer lines start to overlap as a consequence of the curvature of the Ewald sphere. An additional advantage is that it is also possible in this case to perform a radial integration over the full area of the two dimensional detector, thus considerably increasing the statistics. This allows one to study the low angle range where (concentration dependent) interparticle scattering weakly contributes to the scattering intensity.

Results

The protein tubulin was purified from pig brains and prepared for experiments as described elsewhere [13]. The samples were assembled and aligned in a 9 T magnetic field before being transported to the SAXS beamline. For these experiments, station 2.1

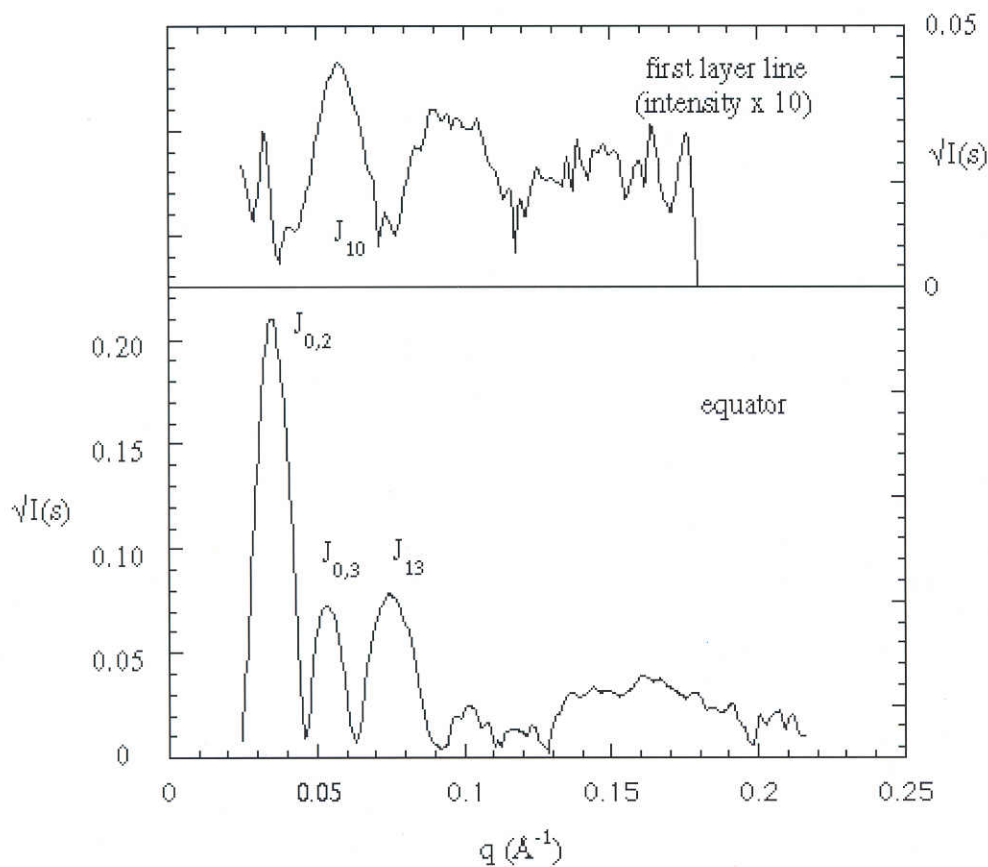


Figure 1: Equatorial and first layer line intensities of the microtubule fibre diffraction pattern. The vertical intensity axis is in arbitrary intensity units. The layer line intensity is weak compared to the equatorial intensity which makes the mathematical correction for the spread in the angular orientation very difficult. For this reason an alternative method of data collection and interpretation was used as described in the text.

of the Daresbury SRS was used. The sample to detector distance was chosen to cover a scattering vector range from $2 \times 10^{-2} < q < 1.8 \times 10^{-1} \text{ \AA}^{-1}$ and $4 \times 10^{-3} < q < 5 \times 10^{-2} \text{ \AA}^{-1}$ respectively.

In Figure 2 the low angle diffraction pattern is shown for a sample aligned with its axis either parallel to or at right angles to the X-ray beam. The radius of gyration of cross section, R_c , can be calculated from the Guinier approximation [14].

$$I(q) = I(0) e^{-\frac{q^2 R_c^2}{2}}$$

For cylindrical scattering objects, R_c is related to the dimensions of the cylinder according to

$$R_c^2 = \frac{R_{outer}^2 + R_{inner}^2}{2} + \frac{h^2}{12}$$

Experimentally it was determined that this value ranged between 167 - 160 \AA . Since the length, h , is, on the scattering range that we're looking at, much too large, it can be assumed that this length will not contribute to the scattering and only the first term remains. If we now take the dimer dimension in the radial direction, i.e. the cylinder wall thickness, to be 65 \AA [1] and thus substituting $R_{inner} = R_{outer} - 65 \text{ \AA}$, we can calculate that the external radius is between 170 - 180 \AA . These values have been used as the

starting parameters in the fitting procedure described below.

Helical diffraction theory [11] tells us that the scattering pattern on the equator of the fibre diffraction pattern can be explained as a combination of a Fourier Transform (FT) of the basic hollow cylinder modulated by cylindrical Bessel functions of the order corresponding with the symmetry in the equatorial plane. This can be approached in two equivalent ways. Either one can use a J_0 Bessel function to describe the cylinder and then convolute this with an unknown function $H(q)$ which represents the shape of the cylinder wall or one can use the FT of a basic hollow cylinder and then add the Bessel function describing these modulations on the basis of intelligent guesses. This has clear analytical advantages. The FT of a smooth walled hollow cylinder is given by [15]:

$$F(q) = R_{outer} \frac{J_1(qR_{outer})}{q} - R_{inner} \frac{J_1(qR_{inner})}{q} \quad [1]$$

The walls of this cylinder will be modulated by electron density grooves between neighbouring protofilaments, both on the inner and outer wall. Due to the 13 fold symmetry these can be expressed as J_{13} Bessel functions with arguments $J_{13}(qR_{inner} + \Delta_{inner})$ and $J_{13}(qR_{outer} - \Delta_{outer})$. The magnitudes of the Δ_{inner} and Δ_{outer} reflect the depth of the grooves on the cylinder wall. It can be calculated that the contribution due to the modulation of the inner wall falls outside the

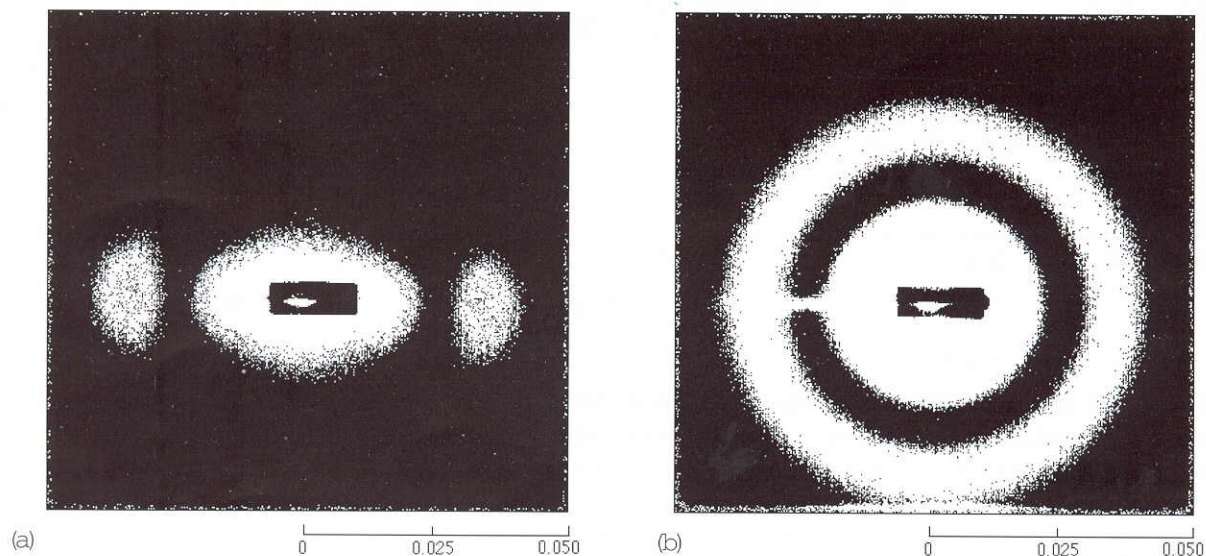


Figure 2: Small angle scattering patterns from microtubules aligned with the long axis at right angles to the X-ray beam (panel a) and with the long axis parallel with the X-ray beam (panel b). The scale is in $q=2\pi/d \text{ (\AA}^{-1}\text{)}$.

scattering range observed in this study, but that the modulation due to the outer wall can add scattered intensity in the observed scattering range at $q > 0.1 \text{ \AA}^{-1}$. An initial fit to the experimental data with an expression based on equation (1) was limited to the range $q < 0.1 \text{ \AA}^{-1}$ and gave $R_{\text{outer}} = 146 \pm 5 \text{ \AA}$ and $R_{\text{inner}} = 86 \pm 5 \text{ \AA}$. The subsequent addition of the contribution of a J_{13} Bessel function relating to the outside wall over a data range that covers the region $q > 0.1 \text{ \AA}^{-1}$ shows that the grooves between the protofilaments are $21 \pm 3 \text{ \AA}$ deep. The results of this fitting procedure are shown in figure 3.

The first layer line can be found on a line with a meridional q -value of $\approx 0.157 \text{ \AA}^{-1}$. As mentioned in the introduction, the degree of alignment is not extremely high and this means that in the equatorial q -range above 0.157 \AA^{-1} it is possible that reflections will start to overlap. However, by using the method of first determining the accurate intensities at lower q on the equator and then fitting these with the appropriate analytical functions, it is possible to deconvolute the intensities coming from layer lines. In fact it might be better, once the equatorial diffraction pattern is accurately determined, to revert back to scattering from randomly oriented samples for the deconvolution procedure. This method is being investigated at the moment.

Figure 4 shows the low angle scattering pattern from three different tubulin concentrations obtained from samples in which the long microtubule axis was coincident with the X-ray beam. The insert shows the very low angle data, where the effects of interparticle scattering are visible. For this concentration range the (theoretical) interparticle distance has been calculated to be varying from 1800 - 2600 \AA which means that it is in the dilute regime according to the definitions of [16]. To gain a better insight into these interparticle effects, simulations were performed by considering the sample to be a two-dimensional disordered fluid, which in this case is allowed due to the molecular axis being aligned. The microtubules were represented as hard, hollow discs with an inner radius of 86 \AA and outer radius of 146 \AA . These discs were randomly placed in a square box of side 10,000 \AA . The packing of N discs into the box was carried out under the constraint that the distance between the centres of any two discs n and m in the box was $r_{nm} \geq 286 \text{ \AA}$, in order to avoid unphysical overlap. The initial configuration of the discs in the box was changed by forcing each disc to undergo random displacements with maximum amplitude of 16 \AA . The displacement was accepted when no overlap with other discs occurred and a new configuration

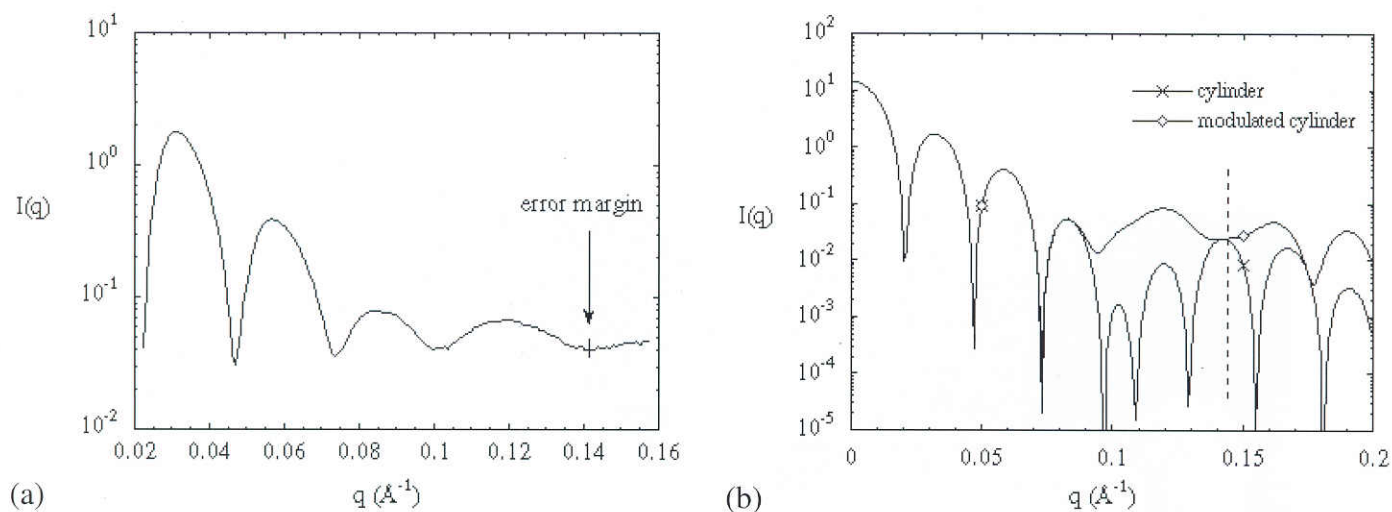


Figure 3: Scattered intensity from microtubules aligned with their long axes parallel to the X-ray beam (panel a). This is equivalent to the equatorial data obtained from a fibre diffraction pattern, but one is certain that neither systematic errors due to mathematical procedures used for correction of the angular spread of the molecules are seen nor intensity due to overlap from diffraction arcs of the layer lines. Panel b shows the best fits ($\chi^2 = 0.05$) to the data using the fitting procedure described in the text. The dotted line indicates the maximum extent of the experimental data at present. The line indicated with 'cylinder' is the contribution of two J_1 functions describing the basic cylinder. The 'modulated' curve is the real fit taking into account the modulations on the cylinder surface.

was produced. Up to 16 000 configurations were used and the diffracted intensity I_L was determined using the positions of the centres of the discs for every fifth configuration. I_L was calculated using the expression

$$I_L(\vec{q}) = I_D(\vec{q}) \sum_{n,m} \exp[-i\vec{q} \cdot \vec{r}]$$

where I_D is the scattered intensity from single hollow discs and q is the wave vector. We evaluated the scattered intensities from configurations containing between 50 and 700 discs, covering an average nearest centre-to-centre distance between 1000 Å and 330 Å. The number of configurations used was chosen judiciously so as to yield statistical fluctuations of less than 3% in the diffracted intensity. The differences in the simulated intensities between different concentrations are approximately a factor of 5 less than the experimental values shown in the insert of Figure 4. This can indicate that the average distance distribution is deviating from that of a completely random distribution and that actually bundles of microtubule polymers are formed. In such a scenario the interparticle scatter will be dominated by the distance distribution inside such a bundle,

apparently giving a much stronger concentration effect.

Conclusions

Helical diffraction theory in combination with experiments on suitably oriented molecules allows us to introduce a step wise fitting procedure with which we first can use knowledge of the basic cylindrical structure of the molecule, then add the Bessel function terms relating to the modulations on the cylindrical surface. Thus we can overcome some problems due to the relatively poor orientation of the molecules [16].

Modelling studies describing the interparticle interference effects are being carried out at the moment. They show qualitative agreement with the experimental data, but give a strong indication that the microtubules are not randomly positioned in the samples but are forming larger bundles.

Liz Towns-Andrews and Sue Slawson of CCLRC Daresbury Laboratory have been very helpful with the fibre diffraction experiments. Joan Bordas is thanked for a useful discussion on the cylindrical nature of the microtubules.

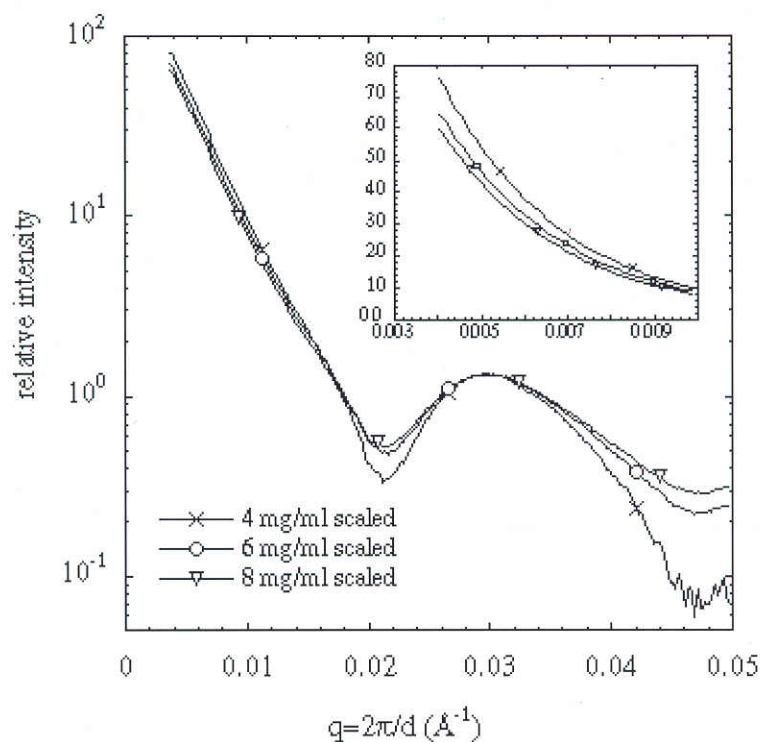


Figure 4: The low angle scattering pattern from microtubules aligned with their long axes parallel to the incident beam for 3 different concentrations. The insert is a magnification of the lowest q -range (with a linear abscissa) showing the effects of interparticle scattering. This effect is much stronger than found in simulated data. This possibly can be due to a non-random distribution of polymers in the samples through clustering in bundles. This will give rise to a locally higher concentration.

References

- [1] *Structure of microtubules* (Eds K.Roberts and J.S Hyams) (Academic Press).
- [2] Gittes, F., Mickey, B., Nettleton, J. and Howard, J., *J. of Cell Biol.* (1993) **120(4)**, 923-934.
- [3] Venier, P., Maggs, A.C., Carlier, M.F. and Pantaloni, D., *J. Biol. Chem.* (1994) **269(18)**, 13353-13360.
- [4] Pirollet, F., Job, D., Margolis, R. and Garel, J., *EMBO journal* (1987) **6(11)**, 3247-3252.
- [5] Mandelkow, E., *Methods in Enzymology* (1986) **134**, 149-168.
- [6] Suzuki, A., Maeda, T. and Ito, T., *Biophys. J.* (1991) **59**, 25-30.
- [7] Flory, P.J., *Proc. Royal. Soc. London* (1956) **A234**, 73-89.
- [8] Bras, W., Diakun, G.P., Díaz, J.F., Maret, G., Kramer, H., Bordas, J. and Medrano, F.J., *Biophysical Journal* (1998) **74(3)**, 1509-1521.
- [9] <http://www.dl.ac.uk/SRS/CCP13>
- [10] Denny, R.C., CCLRC Daresbury laboratory private communication.
- [11] Klug, A., Crick, F. and Wyckoff, H., *Acta. Cryst.* (1958) **11**, 199-213.
- [12] Amos, L.A. and Klug, A., *J. Cell. Sci.* (1974) **14**, 523-549.
- [13] Andreu, J.M., Bordas, J., Díaz, J.F., Garcia de Ancos, J., Gil, R., Medrano, F.J., Nogales, E., Pantos, E. and Towns-Andrews, E., *J. Mol. Biol.* (1992) **226**, 169-184.
- [14] Glatter, O., in *Small Angle X-ray scattering* (Eds Glatter, O. and Kratky, O.) (Academic Press, 1982).
- [15] Vainshtein, B.K., in *Diffraction of X-rays by chain molecules* (Elsevier, 1966).
- [16] Edwards, S.F., *Proc. Phys. Soc.* (1966) **88**, 265-281.

* A part of the problem due to the poor orientation might be overcome by keeping the samples during the experiments in a magnetic field. Preparations, in collaboration with the High Magnetic Field Laboratory (Grenoble), to use a 10 T split coil magnet are in an advanced state. Interested people can contact W. Bras.

The ups and downs of native cellulose structure

R.P. Millane

Whistler Center for Carbohydrate Research and Computational Science and Engineering Program, Purdue University, West Lafayette, Indiana 47907-1160, U.S.A.

Cellulose was one of the first materials to be studied by X-ray fibre diffraction. Although structural studies have continued over the last 60 years, ambiguities have persisted with regard to chain packing and multiple phases of native cellulose, and only recently have these been resolved. X-ray fibre diffraction has played a dominant role, although other techniques have also provided essential information.

Cellulose is the major constituent of most land plants, is the most abundant natural compound, and is an important commercial raw material. It is a linear polymer of 1→4-linked β-D-glucose with a degree of polymerisation >3000. In native cellulose, the molecules are aligned to form fibres, some regions of which have an ordered crystalline structure. The crystalline regions vary in size, are mechanically strong, and are resistant to chemical and enzymatic attack. Cellulose is a structural component in plant and other systems and is used widely in industry. Artificial cellulose derivatives are also used extensively in a variety of industries. Although plant sources are the most familiar, cellulose is also present in bacteria, fungi and algae. Due to its ubiquity and importance, and its polycrystalline nature, cellulose was one of the first materials to be studied by X-ray fibre diffraction analysis. The first such studies were reported by Meyer and Misch [1] in 1937, on plant cellulose from ramie. They determined that the unit cell is monoclinic, that two molecules pass through the unit cell, and suggested that the chains have two-fold screw symmetry. Further studies, including data from electron diffraction and infrared spectroscopy, and also from algal celluloses, supported the results of Meyer and Misch, but with some differences [2-4]. Most notably, diffraction patterns from the algal celluloses contained a few, extra, weak reflections. These were attributed to the *a* and *b* unit cell dimensions being twice those of the plant celluloses. This "large" unit cell therefore contains eight molecules, and there were presumably small differences between the packing and/or molecular